J. Fluid Mech. (1992), *vol.* 244, *pp.* 547–566

Exponential tails and skewness of density-gradient probability density functions in stably stratified turbulence

By S. T. THORODDSEN AND C. W. VAN ATTA†

Applied Mechanics and Engineering Sciences, 0411, University of California, San Diego, La Jolla, CA 92093, USA

(Received 20 September 1991 and in revised form 6 March 1992)

We have measured the probability density functions (PDFs) of density fluctuations and of density-gradient fluctuations in decaying stratified turbulence, using a thermally stratified wind tunnel. The turbulence was generated by passing the flow through a biplanar grid at the entrance to the test section. The linear mean vertical temperature gradient could be adjusted to produce different stratification strengths. The PDFs of the density-gradient fluctuations exhibit extended exponential tails, while those for the density fluctuations are nearly Gaussian. As the turbulence decays away from the grid the exponential tails of the density gradient PDFs become steeper and the central rounded part of the distribution widens. The tail steepness scales approximately as $Re_\lambda^{-\frac{1}{2}}$. Buoyancy forces are not the cause of the exponential tails, since when normalized in r.m.s. units the behaviour of the tails is independent of stratification strength. The vertical temperature gradients $\partial\theta/\partial z$ (measured using two cold wires) show a strong positive skewness close to the grid where the turbulence is most vigorous. This skewness is not caused by non-Boussinesq effects and is present for all stratification strengths. We propose a simple phenomenological model (similar to that of Budwig *et al.* 1985), based on stirring of fluid parcels advected in the mean gradient, to explain the presence of this skewness. The skewness observed by other researchers and their interpretations are discussed in the context of this model. The buoyancy flux PDF also shows strong exponential tails and is very strongly skewed. Both of these properties are consistent with joint-Gaussian statistics of the vertical velocity and temperature fluctuations.

1. Introduction

The probability density functions (PDFs) of random variables are important in statistical mechanics as an accurate estimate of the PDF defines all the moments of the signal. PDfs and especially their tails are also important for predicting extrema. There is at present a renewed interest in the PDFs of various turbulent quantities. Despite the fact that the velocity fluctuations in homogeneous turbulence have been shown to be closely Gaussian, see Townsend (1947), Van Atta & Chen (1968) and others, it has been known for some time that many other turbulent quantities of dynamical interest show non-Gaussian behaviour. Many studies of turbulence, beginning with Townsend (1947), have shown the essential dynamical role of the non-Gaussian behaviour of $\partial u/\partial x$, manifested by Reynolds-number-dependent skewness and flatness factors as compiled by Van Atta & Antonia (1980). Velocity-gradient

† Also at Scripps Institution of Oceanography.

statistics are at the heart of the non-linear dynamics of turbulence and the skewness of $\partial u/\partial x$ is connected with the energy transfer to small scales by vortex stretching, as first shown by Taylor (1938). Van Atta & Chen (1970) found that the PDF of $\partial u/\partial x$, for very large-Reynolds-number atmospheric data, exhibited extended exponential tails. More recently Yamamoto & Hosokawa (1988) found that the PDF of the vorticity magnitude, obtained from a numerical simulation of decaying isotropic turbulence, also has exponential tails. Experimental results of Castaing *et al.* (1989) from thermal convection at very high Rayleigh numbers have also shown temperature fluctuations whose PDFs have exponential tails in the 'hard turbulence' regime. Non-Gaussian statistics with extended probability-density tails have also been observed in surface pressure fluctuations measured in environmental wind tunnels (Peterka & Cermak 1975) and play an important role in predicting extreme wind loads.

Numerical simulations of turbulent thermal convection by Balachandar & Sirovich (1991) have shown strong persistence of exponential tails both in temperature gradients and velocity gradients as well as 'superextended skirts' for the PDFs of the second derivatives of these quantities and of vorticity components.

Numerical simulations of turbulence in a stably stratified fluid have recently included calculations of some PDFs. Using large-eddy simulations and direct numerical simulations Métais & Lesieur (1992) have found extended exponential tails in scalar gradients as well as in pressure fluctuations. Similar direct Navier–Stokes simulations by Gerz & Schumann (1991) also provide results for the skewness of temperature gradients relevant to our present experimental data.

The recent experimental and computational results have been paralleled by theoretical work aimed at explaining the persistence of exponential tails in various turbulent quantities, including work by Kraichnan (1974, 1990), Sinai & Yakhot (1989), Yakhot (1989), Benzi *et al.* (1991) and Pumir, Shraiman & Siggia (1991). Using a multifractal approach Benzi *et al.* predict the PDF of velocity gradients to be a superposition of stretched exponentials, corresponding to the various singularity exponents. Pumir *et al.* suggest that exponential tails are generic to scalar fluctuations in a certain class of turbulent flows including random advection and mixing of the scalar in a background mean scalar gradient, with no requirement of a large separation of scales or strong nonlinear Navier–Stokes transfer. Most recently, Jensen, Paladin & Vulpiani (1992) have introduced a shell model for the small-scale statistics of passive scalars in turbulent fluids.

She (1991) has developed a physical model that succeeds very well in describing the extended tails of PDFs of transverse velocity gradients.

Experiments of the type carried out by the present authors to investigate mixing in stably stratified turbulence, e.g. Thoroddsen & Van Atta (1992), contain the principal ingredients mentioned in the above theories and provide a generically simple well-controlled case of passive and active scalar mixing in a mean gradient. This situation is well suited for experimental study of the PDFs of scalar fluctuations and their gradients. We have therefore extended our earlier study to include measurements of such PDFs in the hope of comparing with numerical simulations and some of the theoretical predictions that have been put forward.

We have also briefly looked at second-derivative PDFs to further emphasize the probability tails in the manner of Balachandar & Sirovich (1991).

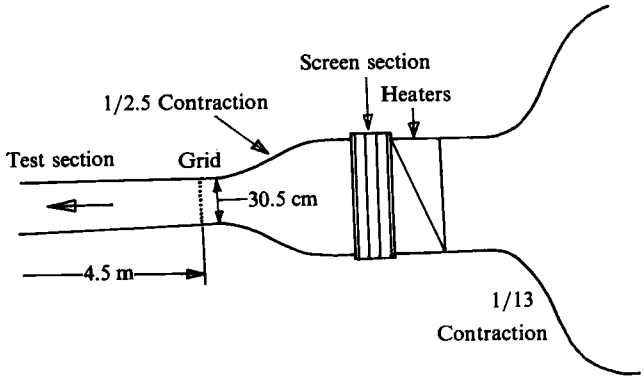

FIGURE 1. Thermally stratified wind tunnel. The mean velocity was in the range 1.7–2.3 m/s.

2. Experiments

2.1. *Thermally stratified wind tunnel*

The thermally stratified wind tunnel used in the experiments is shown in figure 1. Numerous triangular metal fins aligned vertically parallel to the flow direction were electrically heated and the heating could be adjusted to achieve the desired background mean temperature gradients entering the test section. The general design of the tunnel and heating scheme is described in detail by Lienhard & Van Atta (1989). The Brunt–Väisälä frequency, N, characterizes the strength of the stratification and is defined as

$$N = \left(-\frac{g}{\bar{\rho}_0} \frac{\partial \bar{\rho}}{\partial z} \right)^{\frac{1}{2}},$$

where g is the gravitational acceleration and $\bar{\rho}$ is the mean density. N has units of (rad/s). The values of N used in the experiments and the mean temperature gradients ($\mathrm{d}T/\mathrm{d}z$) corresponding to these profiles were 1.25 (48), 2.53 (210), 3.06 (315) and 4.03 rad/s (542 °C/m). For most of the data runs, a biplanar grid made of circular steel rods with 2.54 cm mesh length was placed at the entrance to the test section to generate the turbulent fluctuations, which then decay downstream. The grid solidity was 31 %. The mean velocity profile was uniform, with the mean velocity, U, in the range 1.7–2.3 m/s. The resulting microscale Reynolds number was as high as 40 close behind the grid and Reynolds numbers based on the grid mesh size were in the range 2300–3100 for the 2.54 cm grid. To obtain data for a wider range of Reynolds numbers (§3.3), we used many different grids of various mesh sizes, while keeping the stratification strength fixed at $N = 2.53$ rad/s.

2.2. *Instrumentation*

Cold wires were used to measure the instantaneous temperature. The cold-wire d.c. bridge circuits were built in-house and are described in Haugdahl & Lienhard (1988). The cold wires themselves were made of platinum wire 0.65 μm in diameter and 0.7 mm in length, resulting in a sufficiently large length-to-diameter ratio to capture all of the dynamically important temperature fluctuations, as discussed in Thoroddsen & Van Atta (1992). Taylor's hypothesis was employed to estimate the streamwise gradients (x-direction) and two vertically separated cold wires were used for measuring the vertical (z-direction) instantaneous temperature gradient. The two cold wires used for each set of measurements were selected to have as close to the

same electrical resistance (length) as possible to minimize errors introduced by the difference in their frequency response. The difference in resistance of the two wires was usually less than 5%. The cold wires were oriented horizontally and perpendicular to the mean flow, unless otherwise stated. The data used consisted for the most part of long continuous time series of 409600 samples each. In some cases up to four sequential records of this data length were used for calculations at a given downstream location in the tunnel. The sample rate was 2500 Hz, which was sufficient to resolve the smallest turbulent scales.

2.3. *Derivatives of the temperature signal*

The spatial gradient $\partial\theta/\partial x$ was obtained from the temporal gradient by employing Taylor's hypothesis. The time-derivative of the temperature time series was taken by using Fourier transforms. The Fourier transforms of 4096 sample-long sections of the time series were multiplied by k_i^2 and then inverse transformed. Overlapping data segments were used to avoid end effects. To avoid the errors associated with differentiating the high-frequency noise, a very sharp Kaiser low-pass digital filter was incorporated with cutoff at the frequency where the signal, at each downstream location in the tunnel, reached the background noise level. No other corrections were applied to the derivative measurements. The spatial differencing in the z-direction was performed by a simple finite differencing of the two temperature signals measured by the two cold wires. The vertical separation distance between the wires was measured with a cathetometer as described in Thoroddsen & Van Atta (1992). The separation distance of the wires was kept at around $4\eta_\theta$, where the *Batchelor microscale* is defined as

$$\eta_\theta = (\alpha^3/\epsilon)^{\frac{1}{4}},$$

where α is the thermal diffusivity and ϵ is the rate of dissipation of turbulent kinetic energy.

Second derivatives in the x-direction were also obtained by the Fourier transform. The probe used to measure $\partial^2\theta/\partial z^2$ contained four cold wires equally spaced in the vertical direction so that two sets of three cold wires could thus be selected to calculate the curvature; the results from the two were compared and showed good quantitative agreement.

3. Results

3.1. *General dynamics of decaying stratified turbulence*

The dynamical evolution of the buoyancy flux and velocity lengthscales in the present flow configuration have been elucidated previously by Lienhard & Van Atta (1990) and further details of the statistical character of moments of the temperature and temperature gradients are presented in Thoroddsen & Van Atta (1992). The buoyancy forces reduce vertical motion of fluid elements, converting kinetic energy to potential energy with respect to the background mean density gradient. The inhibition of vertical fluid motion is shown most clearly by the corresponding normalized buoyancy flux, which is shown in figure 2 for the three weaker stratifications. For the strongest stratification the temperature fluctuations in the flow were too large to allow accurate use of hot wires to measure the velocity fluctuations necessary to estimate the flux. The flux behaviour demonstrates that close to the grid where the internal Froude number is largest the flux is essentially that of a passive scalar and is not dependent on buoyancy, but for larger buoyancy

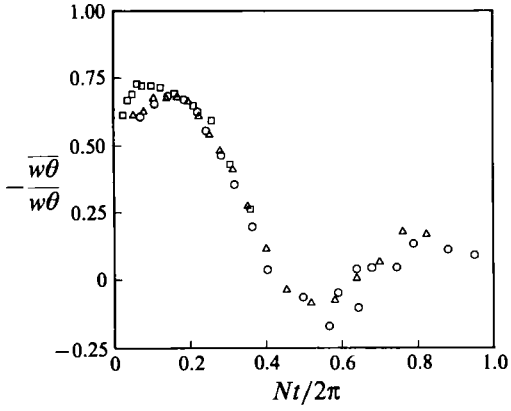

FIGURE 2. Normalized buoyancy flux *vs.* buoyancy time for three different stratification strengths: ○, $N = 3.06$; △, 2.53; □, 1.25 rad/s (from Thoroddsen & Van Atta 1992).

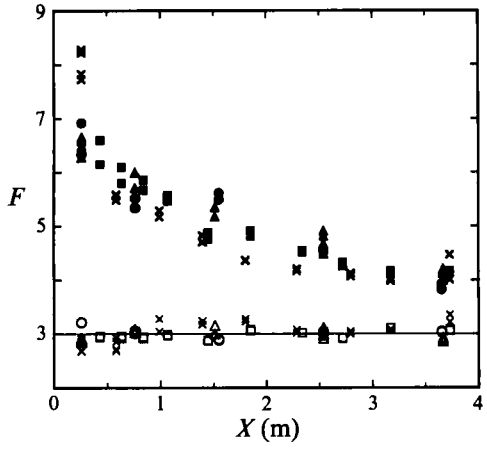

FIGURE 3. Flatness factors of temperature fluctuations (open symbols) and streamwise temperature-gradient fluctuations (filled symbols) *vs.* downstream distance for $N = 1.25$ (□), 2.53 (△), 3.06 (○) and 4.03 rad/s (×). The θ points are clustered around the Gaussian value of 3, while the results for $\partial\theta/\partial x$ show much larger F.

times ($Nt/2\pi \geqslant 0.3$) the stirring is strongly inhibited. The time t represents here the evolution time from the grid, i.e. x/U. The initial passive scalar behaviour can be used as a reference for the importance of buoyancy in what follows.

The flatness factors of a random variable emphasize the spread of its probability density tails. Figure 3 shows the flatness factors of the temperature fluctuations and their streamwise gradients. The flatness of θ is consistently close to the Gaussian value of 3, but the flatness of $\partial\theta/\partial x$ deviates sharply from the Gaussian value, becoming as large as 9 closest to the grid, but then decreases monotonically downstream.

3.2. *Probability density functions of* θ and $\partial\theta/\partial x$

The probability density functions were computed for the temperature and its gradients. In what follows the PDFs have been normalized in r.m.s. units to facilitate comparisons between the results for different stratification strengths, i.e.

$$P(\alpha) = P\left(\frac{\alpha^* - \langle\alpha^*\rangle}{\alpha^*_{\rm rms}}\right),$$

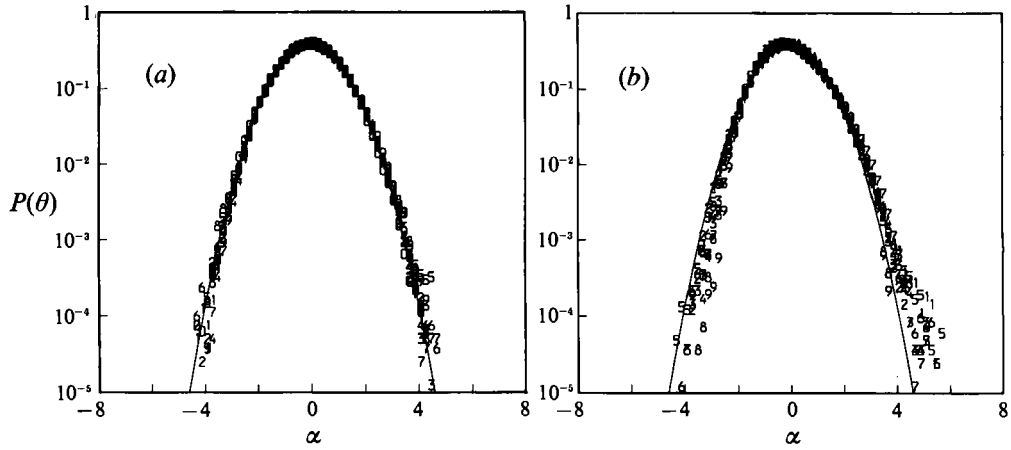

FIGURE 4. PDFs of temperature fluctuations, θ, at many streamwise locations from the grid, for (*a*) $N = 1.25$ rad/s and (*b*) $N = 4.03$ rad/s.

where α^* is the measured temperature fluctuation, θ, or its gradients $\partial\theta/\partial x$ and $\partial\theta/\partial z$. For exponential behaviour of the probability density tails, i.e.

$$P(\alpha) \propto \mathrm{e}^{-D|\alpha|}, \tag{1}$$

the tails will be linear on a log-linear plot of P *vs.* α.

The temperature fluctuations, for all values of N, show close to Gaussian behaviour, with the data for the three weaker stratifications approaching the closest to the Gaussian curve. Figure 4 shows the PDFs for many downstream locations from the grid, for $N = 1.25$ and 4.0 rad/s. The data points follow closely the Gaussian curve for all downstream locations for $N = 1.25$ as well as 2.5 and 3.0 rad/s (not shown here). For the strongest stratification, $N = 4.0$ rad/s, the correspondence with a Gaussian is not quite as good. This may be due to slight deviations from linearity of the mean temperature gradient peculiar to the $N = 4.0$ rad/s case. For this stratification strength the linear section of the mean temperature profile extended only 3 grid mesh sizes (7.6 cm) in the vertical direction at the tunnel centreline, whereas for the other values of N the linear section covered almost the full height of the tunnel. None of the θ-distributions exhibit exponential tails.

In sharp contrast with the near-Gaussian behaviour of the temperature fluctuations, the probability densities of the streamwise gradients of the temperature exhibit strongly exponential behaviour, as shown in figure 5 for the locations closest to the grid where the turbulence is most vigorous. For $N = 2.53$ rad/s the exponential tails extend over almost all of the parameter range. The distributions for $N = 1.25$ and 3.0 rad/s (not shown here) look identical. The distribution for the strongest stratification, shown in figure 5(*b*), differs somewhat from the other cases, showing an extruded peak for small absolute values. Similar peaky probability distribution shapes have been noted for scalar and velocity gradients in experimental and computational studies by Van Atta & Chen (1970), Antonia *et al.* (1984), She (1991) and Balachandar & Sirovich (1991). A related kind of peaky distribution shape has also been derived for θ from numerical studies of Lagrangian turbulence in simple deterministic flows by Goldhirsch & Yakhot (1990).

Further downstream, as the turbulence decays away from the grid, the tails grow progressively steeper, but retain their exponential behaviour, even at the largest

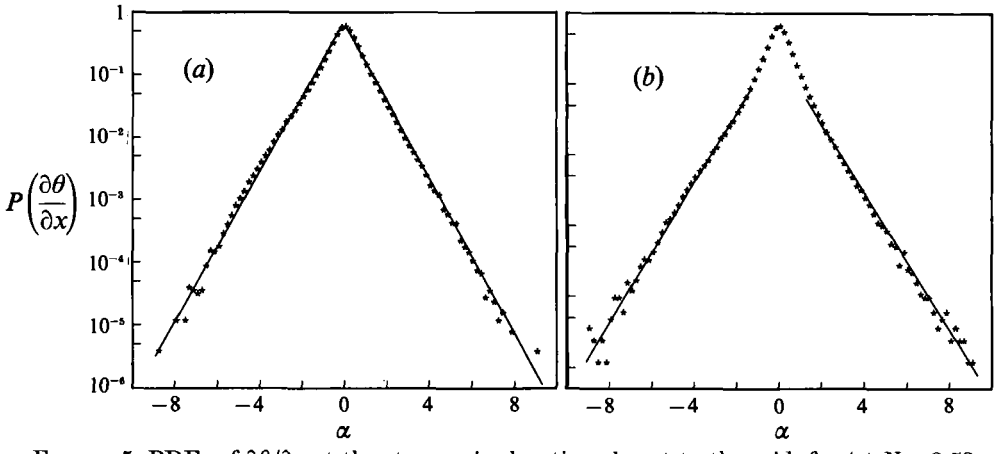

FIGURE 5. PDFs of $\partial\theta/\partial x$ at the streamwise location closest to the grid, for (*a*) $N = 2.53$ and (*b*) $N = 4.03$ rad/s.

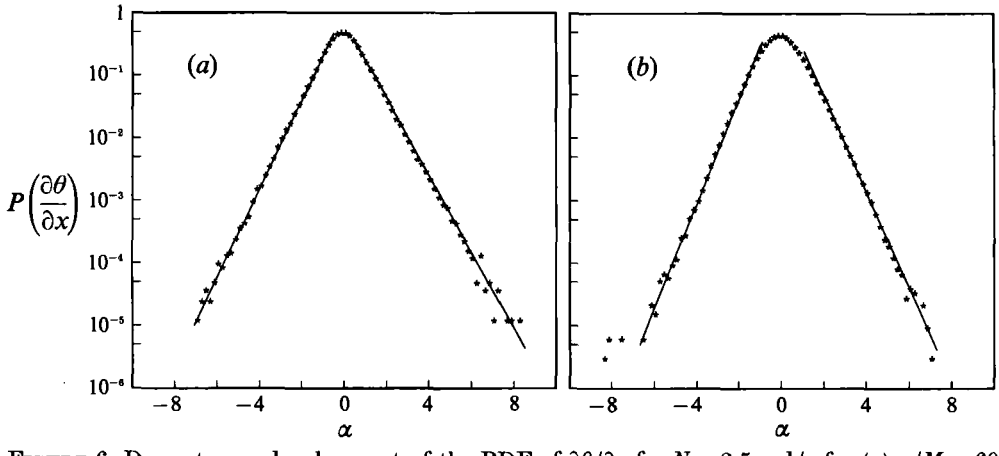

FIGURE 6. Downstream development of the PDF of $\partial\theta/\partial x$ for $N = 2.5$ rad/s for (*a*) $x/M = 60$ and (*b*) 145. Figure 5(*a*) shows corresponding PDF for $x/M = 10$.

x-values, as is shown by comparing figures 5(*a*) and 6(*a*, *b*) for the $N = 2.5$ rad/s stratification. The results for other N, not shown here, are very similar. For small absolute values the distribution widens.

3.3. *Downstream development of the tail steepness*

Least-square linear fits to the probability density tails, shown in the previous section, were computed to investigate the changes in the normalized steepness, D in (1), with the turbulent decay and the changes in stratification. Figure 7 shows the slopes plotted *vs.* evolution time x/U for all stratifications. The slope of the tails increases downstream, with the tails coming closer to the Gaussian shape, by 'folding onto it'. This 'folding behaviour' can be explained by the following argument. The largest gradients, forming the extrema of the tails, are associated with the smallest scales, i.e. small linear dimensions between two fluid volumes of very different temperatures, either due to shear zones at the boundaries of larger colliding eddies or wisps of fluid carried far away in the background gradient. These large-gradient regions are the regions most strongly affected by the diffusion of the scalar, which

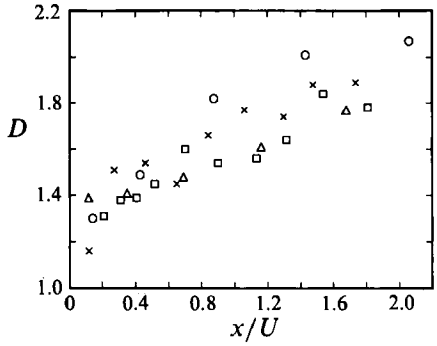

FIGURE 7. The PDF slope, D in (1), of the exponential tails for $\partial\theta/\partial x$ *vs.* evolution time for $N = 1.25$ (□), 2.53 (△), 3.06 (○) and 4.03 rad/s (×).

selectively eliminates the largest gradient values. This preferential smoothing of the smallest scales is not compensated for by scaling the PDF with the r.m.s. since most of the contribution to the r.m.s. is associated with larger scales. The lack of strong generation of new gradients is an indication of reduction in the nonlinear vertical transfer of fluid elements due to reduction in turbulent Reynolds number. Buoyancy forces do not affect the steepness directly, as demonstrated by the very similar slope development for the widely different stratification strengths represented by the data shown in figure 7.

Tail slope, D, vs. Re_λ

To further investigate the evolution of D with Reynolds number we used data that were collected using widely different grid mesh sizes, for a fixed stratification strength, $N = 2.53$ rad/s. The four different grid mesh sizes used were 0.635, 1.27, 2.54 and 5.08 cm. The resulting turbulence spanned a wide range of turbulent Reynolds numbers, defined as

$$Re_\lambda = u'\lambda/\nu,$$

where the lengthscale λ is the Taylor microscale. For these experiments the cold wire was vertically oriented. Since the PDFs for $\partial\theta/\partial x$ show small skewness, the average of D from both the positive and negative tails was used.

Dimensional analysis (Tennekes & Lumley 1972) suggests that the turbulent Reynolds number should be constant for grid turbulence irrespective of the streamwise location, but in practice Re_λ is largest close to the grid and then diminishes rapidly to an approximately constant level farther downstream. This produces the range of Re_λ for each mesh size, as shown in figure 8, which shows D for all mesh sizes and all downstream locations. For comparison the figure also contains an approximate estimate of the slope observed by Antonia *et al.* (1984) for flow of much larger Reynolds number in a heated jet, which yields a significantly smaller values of D. The data in figure 8 follow fairly well the relation

$$D \propto Re_\lambda^{-\frac{1}{2}}. \tag{2}$$

The data of Van Atta & Chen (1970) for $\partial u/\partial x$ in high-Reynolds-number atmospheric turbulence similarly showed D-values of approximately 0.5. The lower D-values associated with increased Re_λ are due to the increased intermittency for the higher-Reynolds-number turbulence, as is demonstrated by increased flatness factors, see Van Atta & Antonia (1980). A purely exponential distribution has a flatness factor

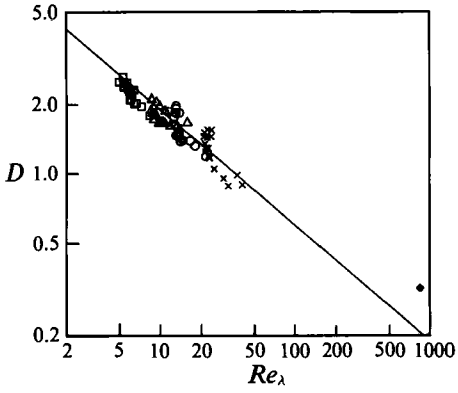

FIGURE 8. Tail steepness D for a wide range of turbulent Reynolds number. The data were all for $N = 2.53$ rad/s and represent different grid mesh sizes, $M = 0.635$ (□), 1.27 (△), 2.54 (○) and 5.08 cm (×); ◆, shows the slope obtained from figure 1 in Antonia *et al.* (1984) for a high-Reynolds-number heated jet.

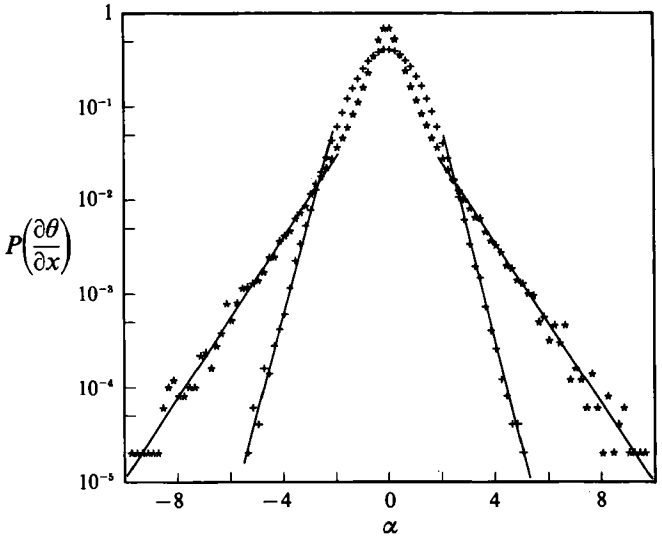

FIGURE 9. PDFs of $\partial\theta/\partial x$ for the two extremes in the Re_λ-range shown in figure 8, $Re_\lambda = 41$ (*) and 5 (+).

of 6, but as shown in figures 3 and 5 (*b*), the higher flatness factors, at larger Reynolds numbers, are associated with a break in the PDF shape, leading to the pointed centre part and more extended tails.

Figure 9 illustrates this change in the PDF shape, showing the PDFs for the largest and smallest Re_λ. The larger the Reynolds number the more extended the tails of the distribution, as discussed above. This is demonstrated even more dramatically by the PDF shown in Antonia *et al.* (1984). Figure 9 clearly demonstrates the persistence of the exponential tails for both the widest and tightest skirts. The difference in shapes is due to the difference in the ratio of the turbulent integral scale to the Batchelor lengthscale, which scales as $Pe^{\frac{3}{4}}$, where Pe is the Péclet number. This affects the competition between diffusion and nonlinear energy transfer. The Péclet number scales linearly with the Reynolds numbers in our case, due to the constant molecular transport coefficients. It could thus replace Re in the forgoing arguments.

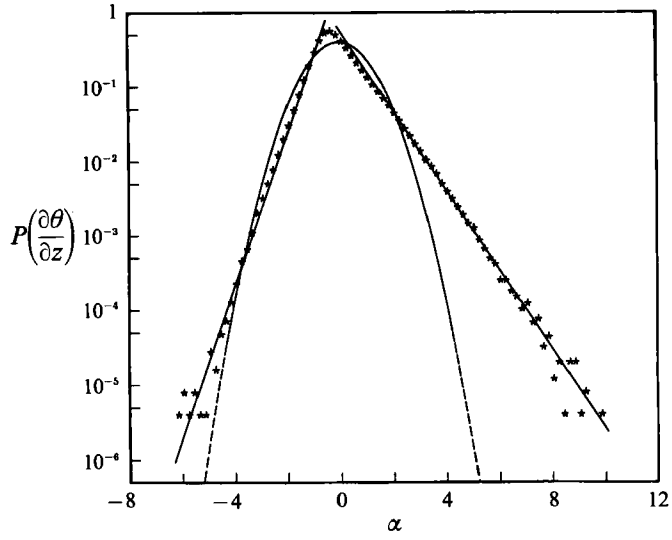

FIGURE 10. PDF of $\partial\theta/\partial z$ closest to the grid for $N = 2.53$ rad/s. The broken line shows the Gaussian PDF.

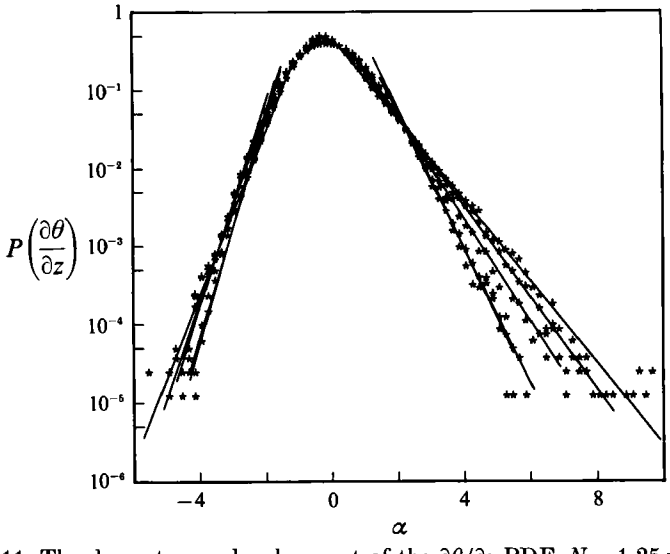

FIGURE 11. The downstream development of the $\partial\theta/\partial z$ PDF, $N = 1.25$ rad/s. The wider tail steepens and the skewness diminishes downstream.

3.4. *PDF and skewness of* $\partial\theta/\partial z$

The PDFs of the fluctuating vertical gradients of θ are also strongly exponential, as shown in figure 10. In contrast with the relatively small skewness of $\partial\theta/\partial x$ the distribution of $\partial\theta/\partial z$ is very strongly skewed. In figure 10 the data are compared with the Gaussian distribution to emphasize the strength of the skewness. The skewness of $\partial\theta/\partial z$ is strong and positive for all N and diminishes downstream with similar retention of the exponential tail shapes as for $\partial\theta/\partial x$. Figure 11 shows the changes in the PDF for a few downstream locations. The wider skirt for positive gradient shows

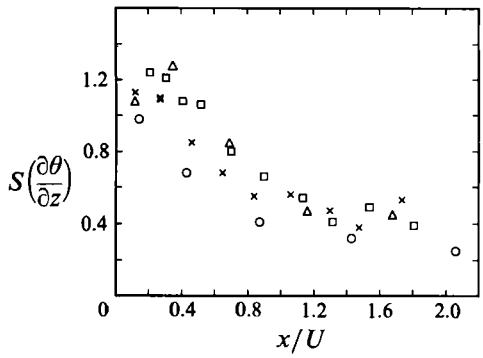

FIGURE 12. Skewness of $\partial\theta/\partial z$ *vs.* downstream location for $N = 1.25$ (□), 2.53 (△), 3.06 (○) and 4.03 rad/s (×).

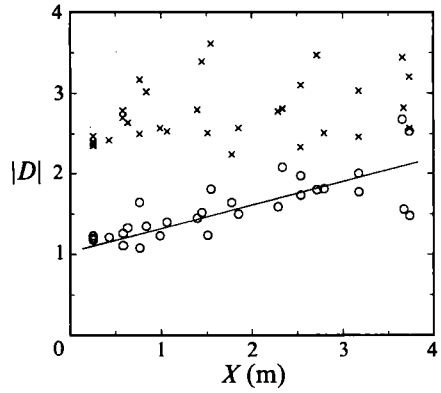

FIGURE 13. Tail slopes of $\partial\theta/\partial z$, D_+ (○) and D_- (×) *vs.* X for many N.

stronger decay, as would be expected by enhanced diffusion of the strongest gradients. Figure 12 shows the downstream development of the $\partial\theta/\partial z$ skewness. The skewness decreases strongly during the initial decay but is independent of buoyancy.

The tail slopes for both sides of the $\partial\theta/\partial z$ PDFs are shown in figure 13. The weaker slopes show a systematic steepening *vs.* x, while the slopes on the steeper side remain nearly constant and show a larger variation, due in part to the larger uncertainty in their determination.

3.5. *PDF of second-order derivatives of* θ

Figure 14 shows the PDFs of $\partial^2\theta/\partial x^2$ and $\partial^2\theta/\partial z^2$ for one case in the passive scalar regime. The figure also contains the PDF of $\partial\theta/\partial x$ and shows that the second derivatives possess wider skirts than the gradient of temperature. The closely Gaussian PDF of θ is also included. Neither the horizontal nor the vertical second derivative show any significant skewness. These results are in agreement with those of the numerical work by Balachandar & Sirovich (1991).

3.6. *PDF of the buoyancy flux*

The PDFs of the temperature fluctuations have been shown in previous sections to be close to Gaussian and, furthermore, so is the PDF of the vertical velocity fluctuations, as shown in figure 15. The probability density of their product $w\theta$, i.e.

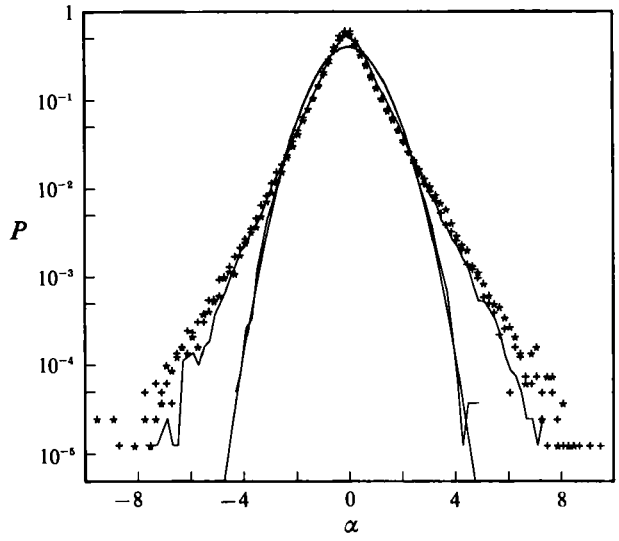

FIGURE 14. PDFs of $\partial^2\theta/\partial x^2$ (*) and $\partial^2\theta/\partial z^2$ (+) for $x/M = 30$ and $N = 2.53$ rad/s. Also included are the PDF of θ falling very close to the Gaussian curve and the PDF of $\partial\theta/\partial x$ (——) showing exponential tails.

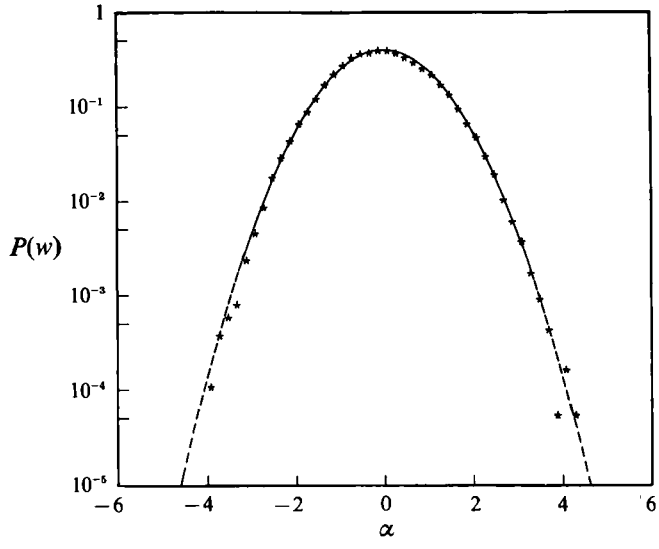

FIGURE 15. PDF of vertical velocity fluctuations w for $N = 2.5$ rad/s at $x/M = 40$.

the instantaneous buoyancy flux $P(w\theta)$, is shown in figure 16 for the strongly mixing regime close to the grid where the buoyancy forces are comparatively small. The distribution exhibits exponential tails and is extremely skewed toward negative values, corresponding to an overall net normalized flux of $\overline{w\theta}/w\theta = -0.68$, with a skewness factor of -2.1 and a flatness factor of 11. The tail slopes D are 0.92 and -3.2.

The PDFs of the temperature fluctuations and the vertical velocity fluctuations are each close to Gaussian. It is therefore interesting to see if the behaviour of $P(w\theta)$ can be derived by assuming joint-Gaussian behaviour of the vertical velocity and temperature fluctuations. We will here follow the notation of Papoulis (1972) and

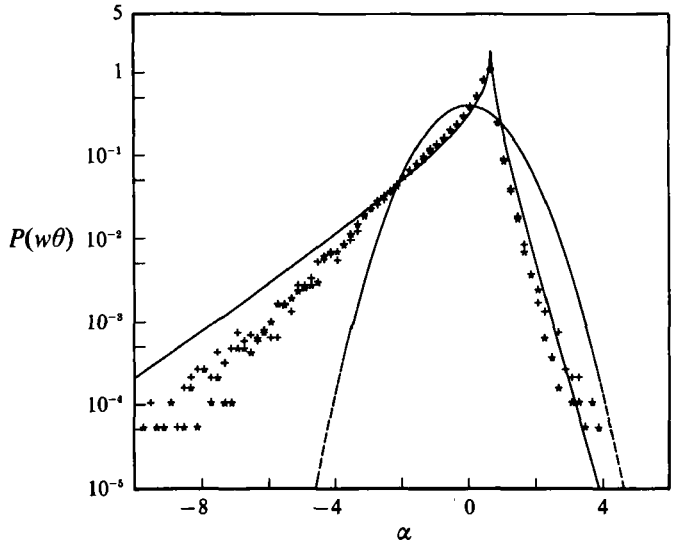

FIGURE 16. PDF of the buoyancy flux corresponding to the PDF of w in figure 15. Included are the Gaussian (----) and the predicted shape (——) from (6) using the measured buoyancy flux correlation value of $r = -0.68$.

derive the form of the PDF of $w\theta$. The joint probability density function of two jointly Gaussian random variables x and y, correlated by a correlation coefficient r has the following form (Papoulis 1972, p. 183):

$$f_{xy}(x,y) = \frac{1}{2\pi\sigma_x\sigma_y(1-r^2)^{\frac{1}{2}}}\exp\left(-\frac{1}{2(1-r^2)}\left(\frac{x^2}{\sigma_x^2}-\frac{2rxy}{\sigma_x\sigma_y}+\frac{y^2}{\sigma_y^2}\right)\right). \tag{3}$$

Let us now define the buoyancy flux variable, i.e. the product of the two random variables, $z = xy$ and look at its cumulative distribution,

$$F_z(z) = \int_{-\infty}^{\infty}\int_{-\infty}^{z/y} f_{xy}(x,y)\,\mathrm{d}x\,\mathrm{d}y. \tag{4}$$

The PDF of z is the derivative of the cumulative distribution,

$$f_z(z) = 2\int_0^{\infty}\frac{1}{y}f_{xy}\left(\frac{z}{y},y\right)\mathrm{d}y.$$

Now by substituting for the distribution f_{xy} from (3) and simplifying we obtain

$$f_z(z) = \frac{1}{\pi\sigma_x\sigma_y(1-r^2)^{\frac{1}{2}}}\exp\left(\frac{rz}{(1-r^2)\sigma_x\sigma_y}\right)\frac{1}{2}\int_0^{\infty}\frac{1}{s}\exp\left(-\frac{1}{2}\left(s+\frac{w^2}{s}\right)\right)\mathrm{d}s, \tag{5}$$

where $w = z/(\sigma_x\sigma_y(1-r^2))$. The integral yields a modified Bessel function of the second kind, $\mathrm{K}_0(w)$, giving the resulting distribution

$$f_z(z) = \frac{1}{\pi\sigma_x\sigma_y(1-r^2)^{\frac{1}{2}}}\exp\left(\frac{rz}{(1-r^2)\sigma_x\sigma_y}\right)\mathrm{K}_0\left(\frac{|z|}{\sigma_x\sigma_y(1-r^2)}\right). \tag{6}$$

The modified Bessel function K_0 has a logarithmic singularity at the origin and for large x-values its asymptotic behaviour is

$$\mathrm{K}_0(x) \approx \frac{\pi}{(2\pi x)^{\frac{1}{2}}}\exp(-x),$$

which produces very close to exponential behaviour. Equation (6), with $r = -0.68$, is compared with the experimental $P(w\theta)$ in figure 16. The agreement is very good except for the largest flux values. For these extreme values, molecular diffusion at the smallest scales may be responsible for decreasing the validity of the joint-Gaussian assumption.

From (6) the normalized ($\sigma_x = \sigma_y = 1$) tail slopes on the two sides of the PDF are predicted as

$$D_{\pm} = \frac{1}{1-r^2}(r \pm 1).$$

The exponential tails of the buoyancy flux distribution, (6), derived here are a consequence simply of the joint-Gaussian statistics of the vertical velocity and temperature as the only assumption. The physics of the fluid stirring and mixing enters the result by determining the value of r.

The distribution of (6) strongly resembles the shape obtained by Kraichnan (1990) for the PDF of $\partial u/\partial x$ in a numerical and analytic treatment of 'turbulence' in Burger's equation.

4. Comparison with results of earlier experiments, numerical simulations and theoretical models

4.1. *Exponential tails*

As mentioned earlier, the observed near-Gaussianity of the temperature fluctuations is not surprising and is consistent with the results of some earlier workers. Here we focus our attention on the essentially exponential behaviour of the tails of the PDFs of both the horizontal and vertical temperature gradients for both passive and active scalar flow regimes. We are aware of no other related experimental results for scalar behaviour in decaying homogeneous turbulence. However, Métais & Lesieur (1992) have recently calculated several PDFs for temperature and temperature gradients in large-eddy simulations and direct numerical simulations for stratified homogeneous decaying turbulence. Their PDFs of temperature fluctuations exhibit weak exponential tails, which we do not see in our measurements, while their PDFs of temperature gradients exhibit much stronger exponential tails, in agreement with our data.

Earlier passive scalar results in other kinds of flows have shown similar exponential behaviour. For a heated turbulent jet ($Re_\lambda = 850$) Antonia *et al.* (1984) found a PDF of temperature close to Gaussian, but the PDF of the temperature differences at closely spaced points exhibited very extended tails. Gollub *et al.* (1992) found weakly exponential tails for temperature, and much stronger exponential tails for temperature gradients in a passive grid-stirring experiment. Their experimental set-up, however, contained essential inhomogeneities, making it hard to generalize the results.

For convectively driven, active scalar mixing Castaing *et al.* (1989) observed exponential tails in PDFs of temperature fluctuations in the 'hard turbulence' regime of Bénard convection, but did not measure temperature gradients. Recently, Ching (1991) reports that PDFs of temperature increments in the same flow exhibit stretched exponential tails. The numerical simulations of Balachandar & Sirovich (1991) for the same regimes of Bénard convection also show strong exponential tails for temperature gradients, but were inconclusive about the PDF of the temperature due to end effects.

No theoretical models have yet appeared for the PDF of the temperature gradients, despite a good deal of theoretical activity stimulated by the Castaing *et al.* (1989) results. The heuristic model of Pumir *et al.* (1991) predicts exponential tails for the PDF of temperature, but gives no prediction for the PDFs of temperature gradients. Our data and the discussion by Pumir *et al.* indicate that their model is not applicable to the temperature field for our experiment. The heuristic arguments of the model cannot in principle be extended to describe the temperature gradient in our experiment. The model requires a non-zero value of the mean gradient of the variable under consideration, and this is zero for our experiment because of the vanishing of the curvature of the mean temperature field, i.e. $\partial^2 T/\partial z^2 = 0$.

The shell model of Jensen *et al.* (1992) predicts PDFs for the temperature increments whose behaviour may approach that of the derivative as the separation distance is decreased. As the distance decreases, the tails of their PDFs become flatter, in agreement with a few calculations of PDFs of increments we have performed. However, there is no indication, in the model results, of an approach to exponential behaviour as the separation distance is decreased.

4.2. *The skewness of* $\partial\theta/\partial z$

The skewness of $\partial\theta/\partial z$ provides a sensitive test of the validity of theoretical models describing turbulent scalar mixing and it is therefore important to quantify.

Budwig, Tavoularis & Corrsin (1985) have measured similar skewness, in an ingenious experiment where they produced the mean temperature gradient by passing the flow through a grid periodically heated to produce a thermal ramp in the streamwise direction. By differentially heating the grid they could also produce a constant transverse temperature gradient. The skewness values thus obtained are qualitatively the same as ours, but differ in the sense that their values grow away from the grids, opposite to ours which decrease away from the grid. This may be due to the difference in heating arrangements used in these two experiments. Budwig *et al.* use two differently sized grids, the first one ($M = 2.54$ cm) to generate the turbulent velocity fluctuations and another set of horizontal nicrome wires (at $x/M = 22$) spaced 0.4 cm part, used to impart the mean temperature gradient. The evolution of the temperature and velocity scales is sensitive to the initial scale ratios as shown by Warhaft & Lumley (1978). This may account for the difference in the development of the skewness, since in our experiments the velocity and temperature fluctuations were generated by the same grid.

Phenomenological model explaining the positive skewness of $\partial\theta/\partial z$

We propose a simple phenomenological model to explain the positive skewness of $\partial\theta/\partial z$, based on the advection of fluid volumes of relatively uniform temperature against the mean temperature gradient. This is illustrated in figure 17, showing how two blobs of fluid advected away from their equilibrium locations will introduce uneven gradients on their two sides in the following manner. If a blob of fluid finds itself in hotter surrounding fluid ($\theta < 0$, for the blob), it is more probable that this blob is moving up in the positive z-direction than down in the negative z-direction, since the $\overline{w\theta}$-correlation is negative. In other words, it is most likely that $w > 0$ since $\theta < 0$. But since this fluid blob is (and has been for some correlation time) moving up through the fluid, it has stirred and mixed with the fluid just below it, spreading out the effective gradient in its wake more than the gradient in the direction of the 'virgin' fluid that it is entering. The $\partial\theta/\partial z$ gradient is thus sharper on the top side of the blob. This is shown schematically in figure 17 (a). Similarly a fluid blob finding

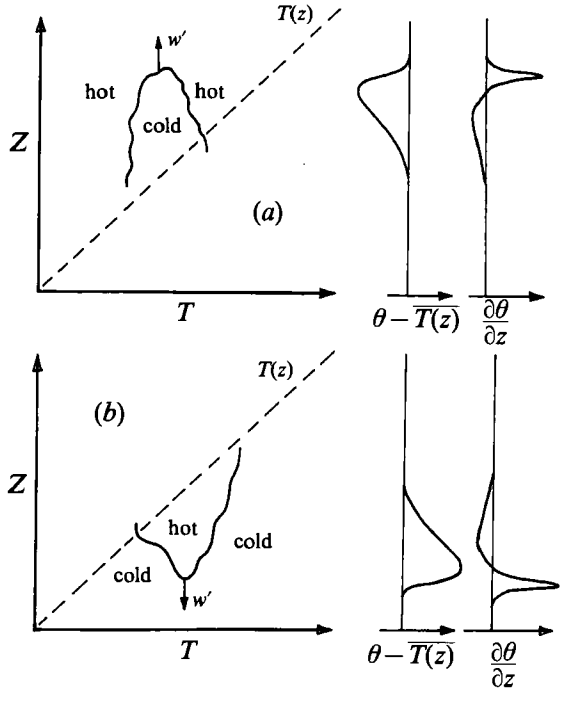

FIGURE 17. Schematic of the simple phenomenological model invoked to explain the measured skewness of $\partial\theta/\partial z$.

itself in colder surrounding fluid ($\theta > 0$) is most probably moving down ($w < 0$) in accordance with the mean flux as explained above. This will in the same manner produce larger gradients on the bottom side of the blob as it moves down into 'virgin fluid' as shown in figure 17 (*b*). Now note that in both of the above-mentioned cases, shown in figure 17, the positive $\partial\theta/\partial z$-gradients are larger than the negative ones, thus introducing a positive skewness. This simple intuitive model thus provides a mechanism biased in favour of larger positive than negative values of $\partial\theta/\partial z$. This breaks the symmetry of $\partial\theta/\partial z$ and predicts the observed sign of the skewness for that quantity, while respecting the following physical properties of the flow: (i) it retains the symmetry of the random advection, i.e. it respects the symmetry and homogeneity of w ($\langle W \rangle = 0$); and (ii) gravity has not been included in the argument, since buoyancy forces are irrelevant, as is born out by the data.

The basic argument for this model is based on the $\overline{w\theta}$-correlation. The fact that the sign of the skewness is not reversed as the turbulence goes through the restratification regime may be explained by the observations of Lienhard & Van Atta (1990) which show that while the largest scales are restratifying there are contributions to the flux at small scales that still produce down-gradient mixing, supplying the required ingredients for the model. The present experiments and model show that the skewness of $\partial\theta/\partial z$ is an inherent property of random advection in a background mean gradient. Notice that the skewness predicted by this model is independent of the magnitude of the mean gradient since the local gradient magnitudes introduced by advection scale linearly with the mean gradient. Note that this model predicts zero skewness for $\partial^2\theta/\partial z^2$ consistent with our measurements and the simulations of Balachandar & Sirovich (1991).

The observed reduction in the skewness away from the grid can be explained in the

following heuristic manner. Close to the grid it is most likely that the large scales of the motion have relatively uniform temperature, since the temperature fluctuations are generated by these large-scale motions imparted by the grid. Farther downstream the stirring will have convoluted this relation of the large-scale blobs, making the blobs a mess of interwoven temperature sheets.

Previous phenomenological models explaining scalar-gradient skewness are due to Tavoularis & Corrsin (1981*b*), Budwig *et al.* (1985) and Balachandar & Sirovich (1991). Tavoularis & Corrsin (1981*b*) have developed an *unified qualitative explanation* of the skewness of $\partial u/\partial x$ and $\partial\theta/\partial x$ for linear shear flows with a linear mean temperature gradient. Their model is based on the existence of a local stagnation region which develops upstream of a fluid 'lump' transported in the positive direction of the mean shear. This model succeeds in explaining the observed sign of the skewness of $\partial u/\partial x$ and $\partial\theta/\partial x$ for the experiments mentioned above. It also predicts the sign of the skewness of $\partial\theta/\partial z$ for a uniform-gradient shear flow, but it predicts erroneously that the skewness of $\partial\theta/\partial z$ is zero for the non-sheared case, i.e. $\mathrm{d}U/\mathrm{d}z = 0$. This model does not invoke mixing or stirring directly, unlike the one we suggest.

Budwig *et al.* (1985) have extended this model to apply to the temperature-gradient skewnesses in their experiments. Their explanations are similar to our model, but they do not directly invoke the mixing. In an interesting side note Budwig *et al.* suggest that their essentially two-dimensional model can explain the skewness of $\partial u/\partial x$, which conventionally is attributed to the three-dimensional mechanism of vortex stretching. Tavoularis, Bennett & Corrsin (1978) have shown that the $\partial u/\partial x$ skewness reduces sharply for $Re_\lambda < 4$.

Balachandar & Sirovich (1991) have also noted $\partial\theta/\partial z$ skewness in their numerical simulations of Rayleigh–Bénard convection. They observed a negative skewness for $\partial\theta/\partial z$ which is consistent with our model, since their mean temperature gradient $\mathrm{d}T/\mathrm{d}z$ was negative, driving the flow. Sirovich (1987) has shown by use of symmetry groups that for the Boussinesq equations $\partial\theta/\partial z$ and $\partial^2\theta/\partial z^2$ are not required to have zero skewness. Balachandar & Sirovich (1991) have presented a skewness model which is similar to ours, in the sense that it is also based on the buoyancy flux correlation, but in their case the buoyancy forces drive the flow and their model invokes the buoyancy-induced acceleration of fluid particles. The skewness is introduced because hot blobs of fluid are accelerated upwards and cold blobs downwards. This leads to a 'peak in their probability distribution at a (small) positive value and this peak is compensated by a less steeper negative tail, in order to yield zero mean value'. This model thus does not directly explain the large negative values of $\partial\theta/\partial z$, but only indirectly through the peak at 'small' positive values of $\partial\theta/\partial z$. This peak at 'small' positive values of $\partial\theta/\partial z$ in turn arises due to the buoyancy flux correlations. Also, since the buoyancy mechanism is essential, the model, like that of Tavoularis & Corrsin (1981*b*), does not predict the observed non-zero skewness of $\partial\theta/\partial z$ for a passive scalar field.

Balachandar & Sirovich's model applies to the observed negative skewness of both $\partial w/\partial z$ and $\partial\theta/\partial z$. It should be pointed out that the negative skewness of $\partial w/\partial z$ is expected for turbulent flows without buoyancy forces, similar to the skewness of $\partial u/\partial x$. From the arguments above it is clear that the $\partial w/\partial z$- and $\partial\theta/\partial z$-skewnesses observed by Balachandar & Sirovich (1991) can be explained without invoking buoyancy forces.

The very similar absolute values of the normalized buoyancy flux for our measurements close to the grid and in the simulated thermal convection suggest

similar dynamics of the turbulent flux, despite the essential difference in the driving mechanism for the two flows. The basis for our simple model can thus be expected to also be applicable to convectively driven flows.

The Gerz & Schumann (1991) pseudo-spectral numerical simulations contain extensive information about the skewness of $\partial\theta/\partial z$ as well as $\partial w/\partial z$ and $\partial u/\partial x$. They attribute the non-zero skewness of $\partial\theta/\partial z$ to nonlinear energy transfer from large to small scales, similar to $\partial u/\partial x$. For small buoyancy times the computed $\partial\theta/\partial z$ skewness value is about 1.1, in good agreement with our measured values. The skewness then decreases with larger buoyancy times to a minimum of 0.3. The passively stratified case shows consistently large skewness, with values as high as 1.5. The initial negative skewness of $\partial w/\partial z$ is similarly reduced to zero due to increased buoyancy forces.

Métais & Lesieur (1992) attribute similar scalar gradient skewnesses in their numerical results to buoyancy forces acting more strongly on the negative gradients than on the positive ones, due to the inherent convective instability of the negative gradients. They do not explain convincingly why this skewness is largest initially for the smallest buoyancy times, where the internal Froude numbers are largest, and then subsequently becomes smaller as the relative strength of buoyancy forces increases.

As mentioned above, our experimental results eliminate buoyancy forces as an essential cause of this skewness, since the experimentally observed skewness is largest close to the grids where buoyancy is weakest and the evolution of the skewness is similar irrespective of the value of N over a large range of stratification strengths.

4.3. *Skewness of $\partial\theta/\partial x$ observed by previous researchers*

Many authors have (when mean velocity shear is present) noted skewness in streamwise derivatives of scalar fluctuations in the direction perpendicular to the mean scalar gradients, i.e. $\partial\theta/\partial x$ in our experiments. This was found only in the presence of mean shear. The scalar is usually temperature in air, thus having the same Prandtl numbers as in the current experiments. Such experiments include both those in very high-Reynolds-number flows in the atmosphere by Gibson, Stegen & Williams (1970), Antonia & Van Atta (1978) and in laboratory flows such as the heated boundary-layer experiments of Sreenivasan, Antonia & Danh (1977). Gibson Friehe & McConnell (1977) have shown that the sign of the skewness changes with the sign of the mean shear. As elucidated by the review of Sreenivasan & Tavoularis (1980) the streamwise skewness is non-zero only when both a mean velocity gradient and a mean temperature gradient are present. Tavoularis & Corrsin (1981*a*, *b*) have further extensively studied the streamwise skewness in shear flows. They derive a model to predict the skewness of $\partial\theta/\partial x$, but their model erroneously predicts that the skewness of $\partial\theta/\partial z \approx 0$ for the limiting case of zero mean shear ($\mathrm{d}\bar{U}/\mathrm{d}z = 0$) as mentioned earlier. This might point to a hidden flaw in this model or suggest some modifications thereto.

Were one to extend our model to homogeneous shear turbulence (say $\mathrm{d}\bar{U}/\mathrm{d}z > 0$) and change the argument to apply to blobs of constant horizontal velocity, instead of temperature, one ends up predicting a positive skewness for $\partial u/\partial z$, as is indeed shown by the measurements of Tavoularis & Corrsin (1981*b*).

5. Conclusions

We have conducted a comprehensive study of PDFs of scalar fluctuations and their gradients in turbulence with a stable mean background scalar gradient. The temperature gradient PDFs exhibit very distinct exponential tails over a wide range of turbulent Reynolds number, while the corresponding PDFs of the temperature fluctuations show close to Gaussian behaviour.

We find that strong buoyancy forces do not alter the exponential behaviour of the PDF tails. The steepness of the tails is a decreasing function of the turbulent Reynolds number and scales approximately as $D \propto Re_\lambda^{-\frac{1}{2}}$ consistent with some data at much higher Reynolds number.

Strong skewness of the $\partial\theta/\partial z$ PDF was observed and predicted by a simple phenomenological model. This model ignores buoyancy forces, consistent with the experimental results, but challenges the interpretations of some previous researchers. The joint-Gaussian statistics of w and θ have been used to predict the highly skewed near-exponential shape of the PDF of the buoyancy flux $w\theta$.

The authors want to thank J. Gollub for stimulating discussions which led to our interest in this problem. We also thank G. Paladin and A. Vulpiani for discussions. This work was supported by ONR Contract no. N00014-86-K-0690 and NSF grant OCE88-17397.

REFERENCES

ANTONIA, R. A., HOPFINGER, E. J., GAGNE, Y. & ANSELMET, F. 1984 Temperature structure functions in turbulent shear flows. *Phys. Rev.* A **30**, 2704–2707.

ANTONIA, R. A. & VAN ATTA, C. W. 1978 Structure functions of temperature fluctuations in turbulent shear flows. *J. Fluid Mech.* **84**, 561–580.

BALACHANDAR, S. & SIROVICH, L. 1991 Probability distribution functions in turbulent convection. *Phys. Fluids* A **3**, 919–927.

BENZI, R., BIFERALE, L., PALADIN, G., VULPIANI, A. & VERGASSOLA, M. 1991 Multifractality in the statistics of the velocity gradients in turbulence. *Phys. Rev. Lett.* **67**, 2299–2302.

BUDWIG, R., TAVOULARIS, S. & CORRSIN, S. 1985 Temperature fluctuations and heat flux in grid-generated isotropic turbulence with streamwise and transverse mean-temperature gradients. *J. Fluid Mech.* **153**, 441–460.

CASTAING, B., GUNARATNE, G., HESLOT, F., KADANOFF, L., LIBCHABER, A., THOMAE, S., WU, X.-Z., ZALESKI, S. & ZANETTI, G. 1989 Scaling of hard thermal turbulence in Rayleigh–Bénard convection. *J. Fluid Mech.* **204**, 1–30.

CHING, E. S. C. 1991 Probabilities for temperature differences in Rayleigh–Bénard convection. *Phys. Rev.* A **44**, 3622–3629.

GERZ, T. & SCHUMANN, U. 1991 Direct simulation of homogeneous turbulence and gravity waves in sheared and unsheared stratified flows. In *Turbulent Shear Flows 7* (ed. F. Durst), pp. 27–45. Springer.

GIBSON, C. H., FRIEHE, C. A. & MCCONNELL, S. O. 1977 Structure of sheared turbulent fields. *Phys. Fluids Suppl.* **20**, S156–S167.

GIBSON, C. H., STEGEN, G. R. & WILLIAMS, R. B. 1970 Statistics of the fine structure of turbulent velocity and temperature fields measured at high Reynolds number. *J. Fluid Mech.* **41**, 153–167.

GOLDHIRSCH, I. & YAKHOT, A. 1990 Probability distribution of a passive scalar: a soluble example. *Phys. Fluids* A **2**, 1303–1305.

GOLLUB, J. P., CLARKE, J., GHARIB, M., LANE, B. & MESQUITA, O. N. 1992 Fluctuations and transport in a stirred fluid with a mean gradient. *Phys. Rev. Lett.* **67**, 3507–3510.

HAUGDAHL, J. & LIENHARD, V, J. H. 1988 A low-cost, high-performance cold-wire bridge. *J. Phys.* E: *Sci. Instrum.* **21**, 167–170.

JENSEN, M. H., PALADIN, G. & VULPIANI, A. 1992 Shell model for turbulent advection of passive scalar fields. *Phys. Rev.* A **45**, 7214–7221.

KRAICHNAN, R. H. 1974 Convection of a passive scalar by a quasi-uniform random straining field. *J. Fluid Mech.* **64**, 737–762.

KRAICHNAN, R. H. 1990 Models of intermittency in hydrodynamic turbulence. *Phys. Rev. Lett.* **65**, 575–578.

LIENHARD, V, J. H. & VAN ATTA, C. W. 1989 Thermally stratifying a wind tunnel for buoyancy influenced flows. *Exps Fluids* **7**, 542–546.

LIENHARD V, J. H. & VAN ATTA, C. W. 1990 The decay of turbulence in thermally stratified flow. *J. Fluid Mech.* **210**, 57–112.

MÉTAIS, M. & LESIEUR, M. 1992 Spectral large-eddy simulation of isotropic and stably stratified turbulence. *J. Fluid Mech.* **239**, 157–194.

PAPOULIS, A. 1972 *Probability, Random Variables, and Stochastic Processes.* McGraw-Hill.

PETERKA, J. A. & CERMAK, J. E. 1975 Wind pressures on buildings – probability densities. *J. Structural Div. ASCE* **101** (ST6), 1255–1267.

PUMIR, A., SHRAIMAN, B. & SIGGIA, E. D. 1991 Exponential tails and random advection. *Phys. Rev. Lett* **66**, 2984–2987.

SHE, Z.-S. 1991 Physical model of intermittency in turbulence. Near-dissipation-range non-Gaussian statistics. *Phys. Rev. Lett.* **66**, 600–603.

SINAI, YA. G. & YAKHOT, V. 1989 Limiting probability distributions of a passive scalar in a random velocity field. *Phys. Rev. Lett.* **63**, 1962–1964.

SIROVICH, L. 1987 Turbulence and the dynamics of coherent structures. Part II. Symmetries and transformations. *Q. Appl. Maths* **45**, 573–582.

SREENIVASAN, K. R., ANTONIA, R. A. & DANH, H. Q. 1977 Temperature dissipation fluctuations in a turbulent boundary layer. *Phys. Fluids* **20**, 1238–1249.

SREENIVASAN, K. R. & TAVOULARIS, S. 1980 On the skewness of the temperature derivative in turbulent flows. *J. Fluid Mech.* **101**, 783–795.

TAVOULARIS, S., BENNETT, J. C. & CORRSIN, S. 1978 Velocity-derivative skewness in small Reynolds number, nearly isotropic turbulence. *J. Fluid Mech.* **88**, 63–69.

TAVOULARIS, S. & CORRSIN, S. 1981*a* Experiments in nearly homogeneous turbulent shear flow with a uniform mean temperature gradient. Part 1. *J. Fluid Mech.* **104**, 311–347.

TAVOULARIS, S. & CORRSIN, S. 1981*b* Experiments in nearly homogeneous turbulent shear flow with a uniform mean temperature gradient. Part 2. The fine structure. *J. Fluid Mech.* **104**, 349–367.

TAYLOR, G. I. 1938 Production and dissipation of vorticity in a turbulent fluid. *Proc. R. Soc. Lond.* A**165**, 15–23.

TENNEKES, H. & LUMLEY, J. L. 1972 *A First Course in Turbulence.* MIT Press.

THORODDSEN, S. T. & VAN ATTA, C. W. 1992 Experiments on anisotropy of density gradients in stably stratified turbulence. *J. Fluid Mech.* (to be submitted).

TOWNSEND, A. A. 1947 The measurement of double and triple correlation derivatives in isotropic turbulence. *Proc. Camb. Phil. Soc.* **43**, 560.

VAN ATTA, C. W. & ANTONIA, R. A. 1980 Reynolds number dependence of skewness and flatness factors of turbulent velocity derivatives. *Phys. Fluids* **23**, 252–257.

VAN ATTA, C. W. & CHEN, W. Y. 1968 Correlation measurements in grid turbulence using digital harmonic analysis. *J. Fluid Mech.* **34**, 497–515.

VAN ATTA, C. W. & CHEN, W. Y. 1970 Structure functions of turbulence in the atmospheric boundary layer over the ocean. *J. Fluid Mech.* **44**, 145–159.

WARHAFT, Z. & LUMLEY, J. L. 1978 An experimental study of the decay of temperature fluctuations in grid-generated turbulence. *J. Fluid Mech.* **88**, 659–684.

YAKHOT, V. 1989 Probability distributions in high-Rayleigh-number Bénard convection. *Phys. Rev. Lett.* **63**, 1965–1967.

YAMAMOTO, K. & HOSOKAWA, I. 1988 A decaying isotropic turbulence pursued by the spectral method. *J. Phys. Soc. Japan* **57**, 1532–1535.